European Journal of Pharmaceutics and Biopharmaceutics 74 (2010) 495–502

Contents lists available at ScienceDirect

European Journal of Pharmaceutics and Biopharmaceutics

journal homepage: www.elsevier.com/locate/ejpb

Research paper

Evaluation of various PAMPA models to identify the most discriminating method for the prediction of BBB permeability

Jurgen Mensch [a,*], Anouche Melis [b], Claire Mackie [b], Geert Verreck [a], Marcus E. Brewster [a], Patrick Augustijns [c]

[a] Chempharm Development, Johnson & Johnson Pharmaceutical Research & Development, A Division of Janssen Pharmaceutica N.V., Beerse, Belgium
[b] ADME-Tox, Johnson&Johnson Pharmaceutical Research & Development, A Division of Janssen Pharmaceutica N.V., Beerse, Belgium
[c] Laboratory for Pharmacotechnology and Biopharmacy, Catholic University Leuven, Leuven, Belgium

ARTICLE INFO

Article history:
Received 28 October 2009
Accepted in revised form 6 January 2010
Available online 11 January 2010

Keywords:
Permeability
Solubility
PAMPA
Caco-2
Efflux ratio
Log BB
Blood–brain barrier

ABSTRACT

The Parallel Artificial Membrane Permeability Assay (PAMPA) has been successfully introduced into the pharmaceutical industry to allow useful predictions of passive oral absorption. Over the last 5 years, researchers have modified the PAMPA such that it can also evaluate passive blood–brain barrier (BBB) permeability. This paper compares the permeability of 19 structurally diverse, commercially available drugs assessed in four different PAMPA models: (1) a PAMPA-BLM (black lipid membrane) model, (2) a PAMPA-DS (Double Sink) model, (3) a PAMPA-BBB model and (4) a PAMPA-BBB-UWL (unstirred water layer) model in order to find the most discriminating method for the prediction of BBB permeability. Both the PAMPA-BBB model and the PAMPA-BLM model accurately identified compounds which pass the BBB (BBB+) and those which poorly penetrate the BBB (BBB−). For these models, BBB+ and BBB− classification ranges, in terms of permeability values, could be defined, offering the opportunity to validate the paradigm with in vivo data.

The PAMPA models were subsequently applied to a set of 14 structurally diverse internal J&J candidates with known log (brain/blood concentration) (Log BB) values. Based on these Log BB values, BBB classifications were established (BBB+: Log BB $\geqslant$ 0; BBB−: Log BB < 0). PAMPA-BLM resulted in three false positive identifications, while PAMPA-BBB misclassified only one compound. Additionally, a Caco-2 assay was performed to determine the efflux ratio of all compounds in the test set. The false positive that occurred in both models was shown to be related to an increased efflux ratio. Both the PAMPA-BLM and the PAMPA-BBB models can be used to predict BBB permeability of compounds in combination with an assay that provides p-gp efflux data, such as the Caco-2 assay.

1. Introduction

The blood–brain barrier (BBB) is a selective barrier formed by endothelial cells that constitute the cerebral microvessels [1–3]. The barrier consists of a network of capillaries in the brain with a total length of 600 km and an average intercapillary distance of 40 μm [4]. The brain endothelium manifests a physical, an efflux and a metabolic barrier to the transport of drugs into the central nervous system. The physical barrier is the result of the tight junctions between endothelial cells, which are 50–100 times tighter than those in capillaries in the periphery [5]. Due to this architecture, exchange of materials between the blood and the brain is dominated by the transcellular route, making the endothelial cells the "gatekeepers" of the brain [5]. The metabolic barrier is provided by several enzymes which are capable of metabolizing drugs and nutrients [6–8]. The presence of various influx/efflux transporters regulates the transcellular traffic facilitating the entry of required nutrients and/or preventing ingress of potentially harmful compounds [9–20]. The main mechanism by which drugs are extruded from the brain is p-gp efflux. Other efflux transporters at the level of the BBB are the multidrug resistance proteins (MRP) and breast cancer resistant proteins (BCRP). Although it is assumed that passive diffusion through the BBB is the most important permeability process, more and more scientists support the idea that carrier-mediated transport and active influx/efflux of drugs are more important than is generally assumed.

While protective in nature, the inability of molecules to permeate the BBB is a significant source of attrition in central nervous system (CNS) drug discovery [21,22]. For this reason, BBB permeability properties of CNS drug candidates should be determined as early as possible in the drug discovery process. In order to assess

* Corresponding author. Chempharm Development, Johnson&Johnson Pharmaceutical Research & Development, A Division of Janssen Pharmaceutica N.V., 2340 Beerse, Belgium. Tel.: +32 14 606320; fax: +32 14 605838.
E-mail address: jmensch@its.jnj.com (J. Mensch).

0939-6411/$ - see front matter © 2010 Elsevier B.V. All rights reserved.
doi:10.1016/j.ejpb.2010.01.003

the potential for small CNS molecules to penetrate the BBB, a variety of methods and models ranging the gamut from in silico to in vivo going through in vitro models have been developed in the hope of generating predictive tools for drug discovery [23,24].

Developments in combinatorial chemistry require that high throughput screening approaches are available for structure–property and structure–permeability assessments. In this context, animal models and associated in vivo studies are not appropriate either at early stages where compound is limited or when compound series need to be evaluated. Therefore, over the past decade, many scientists have been searching for a translational model to assess in vivo BBB drug permeability [25–28]. Traditional methods include cell cultures derived from cerebral (brain capillaries, primary, low passage or immortalized brain endothelial cells) and non-cerebral sources (MDCK, ECV304/C6 cell lines) as well as non-cell based in vitro systems. Unfortunately, most of these methods are complex, time-consuming, costly and unsuitable for screening large numbers of drug candidates. Therefore, in vitro BBB cell culture models are more often used in a later stage of the drug discovery process.

A promising technology to meet the aforementioned needs of CNS drug discovery is the Parallel Artificial Membrane Permeability Assay (PAMPA) first developed as a surrogate for gastrointestinal (GI) absorption. This model is used in the pharmaceutical industry to determine the permeability properties of molecules as soon as possible in drug discovery [29–41]. PAMPA involves non-biological, artificial membranes and thus only focuses on the prediction of passive, transcellular drug absorption. By modifying the lipid composition of the artificial membranes, the system may be capable of predicting CNS permeability with reasonable accuracy [42–44]. A PAMPA model using a porcine brain lipid extract dissolved in *n*-dodecane (2% w/v) as the membrane barrier has been demonstrated to appropriately identify compounds as either BBB permeable (CNS+) or non-permeable (CNS−).

In the present study, the permeability values at pH 7.4 of 19 structurally diverse, commercially available drugs, with known in vivo BBB penetration potential (distribution, in situ perfusion), were assessed using four PAMPA models in order to find the most discriminating method and to establish BBB+ and BBB− permeability ranges. The models applied in this study are: (1) a PAMPA-BLM model using a black lipid membrane and an 18-h incubation time; (2) a PAMPA-DS (Double Sink) model with a gastrointestinal tract (GIT) lipid membrane and a 4-h incubation time; (3) a PAMPA-BBB method with a porcine polar brain lipid (PBL) with an 18-h incubation time and (4) a PAMPA-BBB-UWL method with a porcine PBL, an unstirred water layer of 60 μm and a 1-h incubation time. In Fig. 1, a schematic representation of the various PAMPA models with their associated characteristics is shown. The models performances (i.e., their ability to discriminate BBB+ from BBB− as well as the associated cut-off ranges) were evaluated for a test set of 14J&J CNS compounds with available Log BB values. Based on these Log BB values, the J&J compounds were classified as BBB+ or BBB− compounds (BBB+: Log BB ⩾ 0; BBB−: Log BB < 0) [45]. Additionally, a bidirectional Caco-2 assay was performed to determine the efflux ratio of all compounds examined. The resulting efflux ratio derived is an additional tool that can support, improve and help with the interpretation of the PAMPA results [32,33] by including an estimate of the contribution of p-gp related efflux.

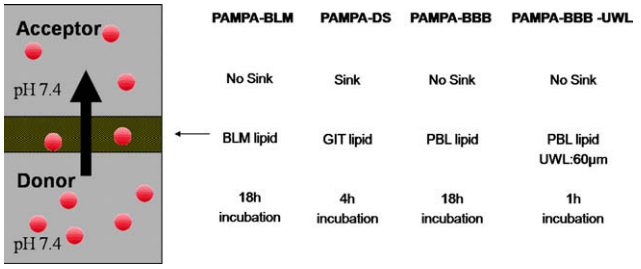

Fig. 1. Representation of experimental conditions and the major differences between the applied PAMPA experiments. BLM: black lipid membrane, GIT: gastrointestinal, PBL: polar brain lipid, UWL: unstirred water layer. (For interpretation of the references to colour in this figure legend, the reader is referred to the web version of this article.)

2. Materials and methods

2.1. Materials

The nineteen commercially available drugs and carbamazepine were obtained from Sigma (Bornem, Belgium) (this training set was used to screen for the most appropriate PAMPA model). Fourteen J&J CNS compounds were obtained from the J&JPRD in-house compound library (Beerse, Belgium) (these drug candidates were applied to the evaluation of the selected PAMPA models and in vivo Log BB experiments and served as the test set of materials). Dodecane and DMSO were sourced from Sigma (Bornem, Belgium). The black lipid membrane (BLM) solution, the gastrointestinal tract (GIT) lipid solution, the system solution concentrate (a proprietary buffer for performing PAMPA), the acceptor sink buffer,(a proprietary acceptor solution for performing Double Sink assays), the PAMPA 96-well sandwiches (a disposable top [with 0.45-μm PVDF filter] and bottom plate), the deep well mixing plates, the V-bottom stock plates, the high sensitivity UV plates, disposable tips, the Gut-Box® (a mechanical stirring apparatus) and coated stirrers were purchased from pION Inc. (Woburn, MA, USA). The porcine polar brain lipid (PBL) was obtained from Avanti Polar Lipids Inc. (Alabaster, AL, USA). Methanol, acetonitrile and formic acid were purchased from Biosolve (Valkenswaard, The Netherlands). Caco-2 cells were obtained from the American Type Culture Collection (ATCC). The culture medium, [Dulbecco's Modified Eagle Medium (DMEM) supplemented with 1% non-essential amino acids (NEAA)], the transport medium, Hanks' balanced salt solution (HBSS) and Trypsin–EDTA were obtained from GIBCO (Carlsbad, CA, USA). MultiScreen® Caco-2 96-well plates (MACAC02S5) and transport plates (MACAC0RS5) were purchased from Millipore (Brussels, Belgium). Culture flasks were obtained from BD Biosciences (Erembodegem, Belgium). Hepes was obtained from Sigma (Bornem, Belgium).

2.2. Determination of thermodynamic solubility

In order to control the precipitation of compounds in the PAMPA experiments, the thermodynamic solubility of the J&J compounds was determined in the universal pION system solution concentrate, adjusted with 0.5 M KOH to a pH 7.4, prior to the PAMPA experiments. Two milliliters of the pION buffer pH 7.4 was saturated with an excess of the J&J compound in a clear glass vial. The mixtures were equilibrated (Edmund Buhler SM25 175 SPM) at ambient temperature overnight and visually inspected thereafter. The resulting suspension was filtered through a 0.45-μM filter tip (disc). An aliquot of the filtrate was diluted (1/10) with an appropriate solvent (0.1 N HCl/acetonitrile, 1/1) and assayed using a generic ultra-performance liquid chromatography (UPLC) method with photodiode array (PDA) detection. Standards were prepared in 0.1 N HCl/acetonitrile, 1/1. When the solubility of a compound was below the detection limit of the generic UPLC method, the samples were re-analyzed with a generic UPLC tandem mass spectrometry method [46]. All PAMPA experiments were conducted at 90% of the maximum solubility of the J&J

compounds to prevent precipitation during the permeability experiments.

2.3. PAMPA-BLM procedure

The PAMPA-BLM (Fig. 1) was performed in a 96-well sandwich plate format similar to that described in the literature [46,47]. A Tecan Genesis robotic system with an eight-probe liquid handling arm was used to perform all solution transfers. The commercially available test compounds were dissolved in DMSO (10 mM) and were subsequently diluted to 200-fold in the pION buffer (pH 7.4) to a final reference concentration of 50 μM. The J&J compounds were dissolved in DMSO to a concentration such that after dilution (factor 200), a final reference concentration of 90% of their thermodynamic solubility in the pION buffer at pH 7.4 was obtained.

The UV spectrum (250–500 nm) of these reference solutions were measured using a 96-well plate reader (Molecular Devices, model 190 Spectramax, Sunnyvale, CA, USA). The pION bottom plate was then filled with the reference solutions to prepare the 'donor' wells. Subsequently, the membranes of a 96-well polyvinylidene fluoride (PVDF) filter (acceptor) plate were coated with 4 μl of the BLM solution, a 2% (wt/v) dodecane solution of dioleoylphosphatidylcholine. All acceptor wells were filled with 200 μl of pION buffer pH 7.4, and the acceptor plate was placed on top of the donor plate to create a "sandwich" in which two compartments were separated by the coated filter. The created "sandwich" was then incubated at 22 °C for approximately 18 h. After this incubation time, the PAMPA sandwich was disassembled and the donor and acceptor solutions were transferred to disposable high sensitivity UV plates (pION Inc., Woburn, MA, USA). The amount of compound in the donor and acceptor wells was determined by UV spectroscopy wherein absorbance between 250 and 500 nm was measured. Previous studies (data not shown) indicated that about 40% of the tested compounds were UV undetectable based on limited sensitivity; therefore, the samples of the PAMPA experiments were also transferred to an Acquity UPLC/MS/MS system (Waters Milford, MA, USA) and analyzed using a generic UPLC/MS/MS method [46]. The PAMPA Evolution software version 2.2 was used to calculate the effective permeability (Eq. (1)) taking into account iso-pH conditions and membrane retention of the drug molecule:

$$P_{\text{eff}} = -\frac{2.303V_d}{A(t-\tau_{\text{lag}})}\left(\frac{1}{1+r_v}\right)\cdot\log_{10}\left[-1+\left(\frac{1+r_v^{-1}}{1-R}\right)\cdot\frac{\text{Ca}(t)}{\text{Cd}(0)}\right] \quad (1)$$

with the aqueous compartment volume ratio, $r_v = \frac{V_d}{V_a}$ (in this case $r_v = 1$), V_d = volume of donor well, V_a = volume in acceptor well, A = filter area, t = permeation time, τ_{lag} = time needed to saturate the membrane, R = mole fraction of solute lost to the membrane, Cd and Ca = concentration in donor and acceptor well, respectively. All compounds were tested in triplicate at pH 7.4, and the average of the three experiments is reported.

2.4. PAMPA-BBB procedure

The PAMPA-BBB model (Fig. 1) applied in this study was based on the BBB model described in literature [44]. The experimental procedure, conditions and P_{eff} calculation of the PAMPA-BBB model were identical to those of the above mentioned PAMPA-BLM model with the exception of the artificial lipid membrane used. The lipid membrane of the PAMPA-BBB model was prepared by dissolving 20 mg of porcine polar brain lipid (PBL) in 1 ml dodecane. The filter membranes of the PAMPA-BBB model were coated with 4 μl of the porcine PBL solution. The lipid composition of this barrier is provided in Table 1. With this setup of identical experimental conditions, the ability of both artificial lipid formulations (BLM vs. PBL) to provide the required BBB classification could be evaluated.

2.5. PAMPA-DS procedure

The PAMPA-Double Sink method (Fig. 1) has become the working standard in the pharmaceutical industry for the prediction of intestinal absorption [48]. In the Double Sink (DS) model [33,36,38,39] applied in this study, surfactant is added to the acceptor buffer (pH 7.4) to create sink conditions by solubilizing lipophilic molecules that have permeated the artificial lipid membrane. For this reason, the permeability equation applied for the PAMPA-BLM and PAMPA-BBB (Eq. (1)) describing the non-sink process is inappropriate for the PAMPA-DS model. In the PAMPA-DS mode, it can be assumed that the reverse transport is effectively zero. Consequently, the permeability equation (Eq. (1)) can be simplified to Eq. (2) [33]:

$$P_{\text{app}} = -\frac{2.303V_d}{A(t-\tau_{\text{lag}})}\cdot\log_{10}\left[\left(\frac{1}{1-R}\right)\cdot\frac{\text{Cd}(t)}{\text{Cd}(0)}\right] \quad (2)$$

The experimental procedure of the PAMPA-DS model is similar to that of the above mentioned PAMPA models, but some experimental conditions are modified. Besides the use of sink conditions in the acceptor compartment, a different artificial lipid solution is applied on the filter membrane (4 μl). This GIT lipid solution (pION Inc., Woburn, MA, USA) consists of 20% soy lecithin dissolved in dodecane. The composition is provided in Table 1. In addition, the incubation time was decreased from 18 h (for PAMPA-BLM and PAMPA-BBB) to 4 h for PAMPA-DS at 22 °C. As a consequence of the addition of the surfactant to the acceptor compartment, the background signal in the mass spectrometer was increased such that no daughter ions could be detected. The use of the surfactant, thus, restricted the analytical possibilities to only UV spectrophotometry.

2.6. PAMPA-BBB-UWL procedure

The in vitro permeability cell culture or PAMPA models can underestimate the true membrane permeability because of the unstirred water layer (UWL) [33]. The in vivo UWL is usually significantly smaller than the UWL associated with an in vitro model. The UWL in the endothelial capillaries of the brain is essentially zero, given that the diameter of the capillaries is about 7 μm and that there is an efficient mixing near the surface due to the passage of blood fluids and erythrocytes [49]. On the other hand, the UWL in an unstirred in vitro permeability cell system can vary from 1500 to 2500 μm.

In the PAMPA-BBB-UWL model (Fig. 1) applied in this study, the UWL of the donor compartment was decreased to 60 μm. All donor wells contained a magnetic-coated stirrer which was individually tumbled by using the GutBox® (pION Inc., Woburn, MA, USA), a mechanical stirring apparatus. The PAMPA-BBB-UWL model used a similar experimental procedure and P_{eff} calculation (Eq. (1)) to those discussed in the PAMPA-BLM and PAMPA-BBB models. In fact, the PAMPA-BBB-UWL model was developed based on the PAMPA-BBB method. In both models, exactly the same artificial lipid solution was prepared by dissolving 20 mg of porcine polar brain lipid (PBL) in 1 ml dodecane. The filter membranes of the PAMPA-BBB-UWL model were also coated with 4 μl of the porcine PBL solution. On the other hand, the differences in experimental conditions compared to the PAMPA-BBB method included the decrease in incubation time to 1 h by using the GutBox® and the resulting UWL of 60 μm.

It can be assumed that the overall resistance to passive transport (inverse of permeability) is the sum of the resistances of the

Table 1
Lipid compositions (w/w) of the artificial membranes used in the PAMPA models. Lipids are dissolved in dodecane: in PAMPA-BLM 2% (w/v) dioleoylphosphatidylcholine; in PAMPA-GIT 20% (w/v) and in PAMPA-BBB 2% (w/v).

Components	PAMPA-BLM	PAMPA-GIT[a]	PAMPA-BBB[a]
Phosphatidylcholine	100	24	12.6
Phosphatidylethanolamine	–	18	33.1
Phosphatidylinositol	–	12	4.1
Phosphatidylserine	–	–	18.5
Phosphatidic acid	–	4	0.8
Lyso-phosphatidylcholine	–	5	
Triglycerides	–	37	
Others (cerebrosides, sulfatides, pigments)	–		30.9

[a] From Avanti Polar lipids (Alabaster, AL, USA).

UWL, on both sides of the membrane (donor and acceptor) and the membrane itself:

$$\frac{1}{P_{\text{eff}}} = \frac{1}{P_u^D} + \frac{1}{P_m} + \frac{1}{P_u^A} \tag{3}$$

where P_m is the permeability of the membrane, P_u^D and P_u^A are the UWL permeability coefficients on the donor and acceptor sides, respectively.

The UWL is characterized by the water diffusivity (D_{aq}) of the drug divided by the thickness of the layer (h):

$$P_u = \frac{D_{\text{aq}}}{h} \tag{4}$$

Reducing the UWL in the donor compartment affects the overall resistance and hence the effective permeability. Because of the vigorous agitation, UWLs smaller than 60 μm resulted in increased variability of P_{eff} among all individual wells.

2.7. Caco-2 bidirectional assay

Caco-2 cells were obtained from the American Type Culture Collection (ATCC) and were used between a passage number of 40 and 60. The cells were maintained in 175-cm^2 plastic culture flasks (BD Biosciences, Erembodegem, Belgium) and were subcultured before reaching confluence. Caco-2 cells were detached with 0.05% trypsin–EDTA (Gibco) for 15 min at 37 °C and seeded in new flasks. The culture medium, Dulbecco's Modified Eagle Medium (DMEM), was supplemented with 1% non-essential amino acids (NEAA). The cells were seeded in 96-well MultiScreen Caco-2 (Millipore, Brussels) at 9000 cells/well and the plates were cultured for 21 days. They were fed basolaterally and apically with 250 μl and 75 μl of fresh medium every other day and were incubated at 37 °C and 5% CO_2. After 7 days, the cells form a full monolayer and, after 21 days, they are fully differentiated and ready for transport experiments.

Prior to the transport experiments, the medium from the basolateral and apical side was replaced with 250 μl and 75 μl of pre-warmed HBSS (25 mM Hepes buffer, pH 7.4), respectively. The plates were allowed to equilibrate for 30 min at 37 °C and 5% CO_2 on a shaker (KS125 basic) at 80 rpm. Subsequently, the integrity of the cell monolayers was determined by the measurement of the transepithelial electrical resistance (TEER). The resistance of the cell monolayers grown on 96-well MultiScreen Caco-2 plates was measured using an Evom resistance voltohm meter (World Precision Instruments, Berlin, Germany). All wells with TEER values less than 200 Ω cm^2 were discarded.

For the apical to basolateral (A–B) transport, the buffer was removed from the cells and replaced with 75 μl of the test compound solution (20 μM) on the apical side while the basolateral compartment was replaced with 250 μl of the pre-warmed HBSS buffer. For the basolateral to apical (B–A) transport, the buffer was removed from the cells and replaced with 250 μl of the test compound solution (20 μM) on the basolateral side while the apical compartment was replaced with 75 μl of the pre-warmed HBSS buffer. The monolayers were incubated for 120 min at 37 °C, 5% CO_2 and shaken at 80 rpm. The amount of drug accumulated in the basal compartment was determined at different time points: 30, 60, 90 and 120 min. At each time point, the entire solution volume from the basolateral side was sampled and replaced with 250 μl of fresh and pre-warmed HBSS buffer for the A–B transport experiments. Likewise for the B–A experiments, the entire volume from the apical side was sampled and replaced with 75 μl of fresh and pre-warmed HBSS buffer. All samples were diluted with acetonitrile (1:1 v/v) prior to analysis with the Acquity UPLC/MS/MS system [46] (Waters Milford, MA, USA). An FDA standard (carbamazepine) was included in all plates as an extra quality control to monitor the consistency of the Caco-2 test. The observed variability of both the A–B and the B–A permeability for carbamazepine was less than 5%.

At the end of the transport experiments, the cell monolayers were rinsed with HBSS buffer and incubated with 75 μl of a sodium fluorescein solution (1 mg/ml HBSS) in the apical compartment and 250 μl HBSS buffer at the basolateral side for an additional 60 min at 37 °C, 5% CO_2 and shaken at 80 rpm. To assess the paracellular transport, 100 μl from the basolateral side was sampled to determine the diffusion of sodium fluorescein into the basal compartment. The diffusion of sodium fluorescein was determined by measuring the fluorescence intensity (excitation 490 nm, emission 514 nm) using a Tecan Genios (Tecan Benelux, Mechelen) fluorimeter.

Final concentrations in the apical and basolateral compartment were quantified by the interpolation of the calibration data. Apparent permeability (P_{app}) values were calculated algebraically:

$$P_{\text{app}} = \left[\frac{\text{amount measured in receiver (μg)}}{\text{area of cells (0.11 cm}^2\text{)} \times \text{duration (7200 s)} \times \text{starting concentration donor (μg/cm}^3\text{)}}\right] \tag{5}$$

Additionally, the efflux ratio could be determined whereby the B–A apparent permeability was divided by the A–B apparent permeability. Compounds with an efflux ratio higher than 2 were categorized as substrates for efflux mechanisms.

2.8. In vivo Log BB experiments

Log BB is the logarithm of the ratio of the steady-state total concentration of a compound in the brain to that in the plasma. The Log BB of the J&J compounds was determined at multiple time points after oral and/or subcutaneous administration to eliminate the time dependence of the resulting brain/plasma ratio. The brain/plasma ratio was then calculated from the areas under the curve (AUC_{brain} in h ng/g; AUC_{plasma} in h ng/ml) for brain and plasma concentrations:

$$\text{Log BB} = \log\left[\frac{AUC_{\text{brain}}}{AUC_{\text{plasma}}}\right] \tag{6}$$

The in vivo brain distribution experiments were part of a larger plasma kinetic and tissue distribution study, and all experiments were carried out in accordance with the EC Directive 86/609/EEC. Three male animals (rats with mean weight 230 ± 9 g) were used per time point, and tap water and food were available ad libitum. In general, samples were taken at 30 min, 1, 2, 4, 7 and 24 h after dose administration. The administered dose varied among the different study protocols between 1 and 40 mg/kg. The dosing formulation was stored at room temperature after preparation, protected from light and analyzed quantitatively with LC–MS/MS on the day of preparation. The stability of the formulation was assessed on the day of dosing.

At each time point, the animals were sacrificed by decapitation and blood was collected by exsanguination into 10-ml BD vacutainers® K3E (Becton Dickinson). Samples were placed immediately on ice, and plasma was obtained following centrifugation at 4 °C for 10 min at approximately 1900*g*. All samples were protected from daylight and stored at ⩽−18 °C prior to analysis. From each animal, individual samples of skin, eye, brain, heart, liver, lung, kidney, muscle and fat were dissected and weighed.

Brain tissue samples were homogenized in demineralized water (1/9 w/v or +3 ml if tissue weight <0.33 g). Homogenization was carried out under controlled light conditions. Plasma and tissue samples were analyzed using a validated research LC–MS/MS method. The Log BB values were then calculated from the areas under the curve for brain and plasma concentrations (Eq. (6)). Generally, compounds with a Log BB greater than or equal to 0 are considered to have sufficient access to the central nervous system and were classified as BBB+ or CNS+; compounds with a Log BB less than 0 are classified as BBB− or CNS−.

3. Results and discussion

3.1. Evaluation of the Caco-2 and PAMPA models to identify BBB permeable or non-permeable model compounds

Nineteen structurally diverse compounds were selected based on their described BBB permeability properties (classified as either BBB+ or BBB−) as cited in the literature [44]. Seventeen of the compounds were reported to penetrate into the brain via passive diffusion. In addition, caffeine (which has been reported to penetrate the brain via both passive diffusion and active transport) and verapamil (a substrate for p-gp efflux) were included in the test set. This test set was assessed with the selected PAMPA methodologies to find the most discriminating model for the prediction of BBB permeability. Furthermore, these compounds were also examined in a bidirectional Caco-2 assay. The permeability results obtained from the PAMPA models and the Caco-2 assessment were evaluated and compared to each other. The results are reported in Table 2 [50–59] and Fig. 2A and B.

The PAMPA-BBB-UWL, PAMPA-DS and the Caco-2 permeability results did not discriminate between the BBB+ and the BBB− compounds. On the other hand, the PAMPA-BBB and the PAMPA-BLM models did separate the BBB+ from the BBB− compounds with the exception of the false negative value for caffeine and the false positive value for verapamil. These results are consistent with the active transport of caffeine by the organic anion transporter [52] and the fact that verapamil is a substrate for p-gp efflux. Both PAMPA-BBB and PAMPA-BLM classified all other compounds correctly as BBB+ or BBB− while PAMPA-BBB was found to have the best discriminating attributes. That is, the PAMPA-BBB method resulted in the largest discrimination range (1.3 vs. 11.1×10^{-6} cm/s) for the selected BBB+ and BBB− compounds (Fig. 2A and B). Based on the obtained permeability data, investigations published in literature [44] and in-house experience, discrimination ranges for both models were defined (Table 3).

Interestingly, as discussed in the experimental section and shown in Fig. 1, the only difference in the experimental setup between the two models (PAMPA-BBB and PAMPA-BLM) is the lipid membrane. While the PAMPA-BBB model uses a more complex porcine brain extract to mimic the blood–brain barrier, the membrane barrier associated with the PAMPA-BLM model, consists of 2% (w/v) dioleoylphosphatidylcholine dissolved in dodecane. To confirm that both models perform well in predicting BBB permeability, the models were tested with a number of J&J drug candidate compounds.

3.2. Evaluation of the PAMPA models using the established classification ranges for a set of J&J compounds

A test set of 14J&J compounds was selected for the evaluations using the defined classification (Table 3) and model robustness. Both in vivo Log BB values after oral (PO) and subcutaneous (SC) administration were obtained in-house. In this way, differences in route of administration could be defined. Based on the in vivo data (Table 4), the J&J compounds were separated into a BBB+ and BBB− category. The Log BB values (Table 4) were plotted as a function of the permeability values obtained from the PAMPA models. Results are shown in Figs. 3 and 4.

The PAMPA-BLM assay, using a 2% (w/v) dioleoylphosphatidylcholine lipid membrane, was found to correctly classify all compounds with the exception of three substances (J&J 9, J&J 12, J&J 13) which were categorized as false positives. This misclassification can possibly be attributed to efflux (Fig. 3). All J&J

Table 2
Literature BBB in vivo penetration classification, PAMPA and Caco-2 results of 19 structurally diverse compounds.

Compounds	Literature BBB+/− classification	PAMPA-BLM P_{eff} (cm/s) 10^{-6}	PAMPA-DS P_{app} (cm/s) 10^{-6}	PAMPA-BBB P_{eff} (cm/s) 10^{-6}	PAMPA-BBB-UWL P_{eff} (cm/s) 10^{-6}	Caco-2 A-B P_{app} (cm/s) 10^{-6}	Caco-2 B-A P_{app} (cm/s) 10^{-6}	Caco-2 efflux ratio
Alprazolam[49]	BBB+	6.62	53.23	11.12	11.48	103.63	106.77	1.03
Atenolol[50]	BBB−	0.00	0.00	0.74	0.00	1.00	1.00	1.00
Caffeine[51a]	BBB+	2.13	2.96	2.03	0.00	44.40	62.16	1.40
Chlorpromazine[52]	BBB+	6.68	114.30	equi	equi	10.70	16.05	1.50
Clonidine[53]	BBB+	3.39	56.27	15.68	0.00	59.90	16.77	0.28
Desipramine[52]	BBB+	Equi	90.40	29.52	equi	16.50	37.95	2.30
Diazepam[49]	BBB+	23.56	83.18	19.32	112.00	65.47	91.65	1.40
Dopamine[54]	BBB−	0.00	2.43	0.54	6.72	–	–	–
Enoxacin[55]	BBB−	0.10	8.98	0.82	0.00	25.00	17.50	0.70
Imipramine[52]	BBB+	27.51	93.70	20.83	equi	37.10	66.78	1.80
Isoxicam[56]	BBB−	0.11	0.50	0.20	0.00	23.20	41.76	1.80
Ofloxacin[55]	BBB−	0.28	24.48	1.27	0.00	9.17	22.00	2.40
Oxazepam[49]	BBB+	2.04	149.50	15.13	134.29	43.63	52.36	1.20
Progesterone[57]	BBB+	15.47	90.60	12.24	67.14	26.63	45.28	1.70
Promazine[52]	BBB+	14.39	80.18	18.35	equi	14.23	27.04	1.90
Tenoxicam[56]	BBB−	0.04	0.79	0.04	1.71	47.43	85.38	1.80
Theophilline[58]	BBB−	0.07	1.49	0.18	0.81	–	–	–
Thiopental[52]	BBB+	20.26	23.88	55.58	23.41	–	–	–
Verapamil[58b]	BBB−	17.58	71.35	23.69	94.68	24.57	51.59	2.10

[a] Caffeine enters the brain by both passive diffusion and active influx. equi: equilibrated concentration of the compound in donor and acceptor compartment and represents high permeable compounds.
[b] Verapamil is a substrate for p-gp and is effluxed from the brain in vivo. (–): no data available.

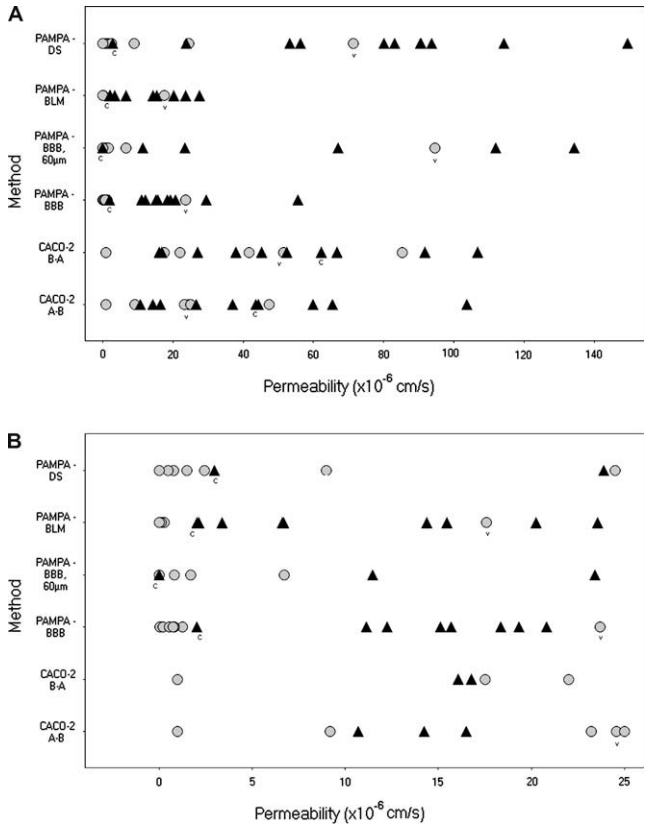

Fig. 2. (A, B) Resulting permeability values of the 19 commercially available compounds obtained with different PAMPA methodologies. Fig. 2B shows the results lower than a permeability value of 26×10^{-6} cm/s. Effective permeability (P_{eff}) values are plotted for PAMPA-BLM, PAMPA-BBB and PAMPA-BBB-UWL. Apparent permeability (P_{app}) are plotted for PAMPA-DS, Caco-2 (A–B) and Caco-2 (B–A). ▲ represent the BBB+ and ● represent the BBB− compounds. (C) Represents caffeine that is known to enter the brain by both passive diffusion and carrier-mediated transport. (V) Represents verapamil that is known as a p-gp substrate and is effluxed from the brain.

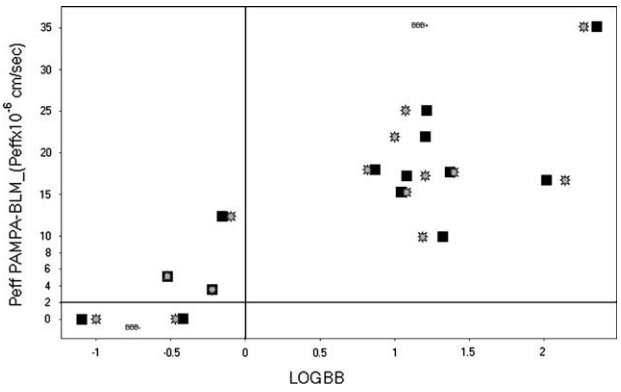

Fig. 3. Log BB values of 14J&J compounds are plotted against the PAMPA-BLM P_{eff} ($\times 10^{-6}$ cm/s) values. ■ represent Log BB values after oral administration and ✲ represent the Log BB values after subcutaneous administration. Based on the indicated classification ranges for PAMPA-BLM, three false positive outliers are obtained.

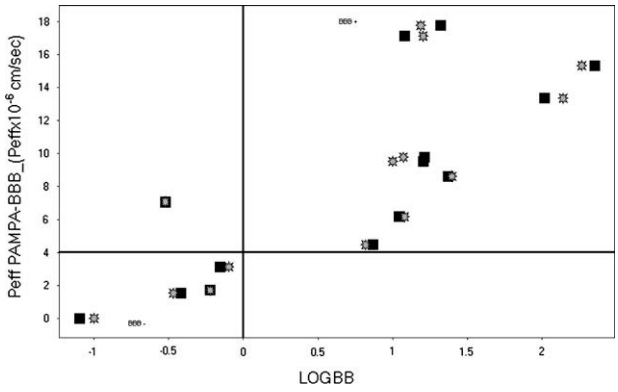

Fig. 4. Log BB values of 14J&J compounds are plotted against the PAMPA-BBB P_{eff} ($\times 10^{-6}$ cm/s) values. ■ represent Log BB values after oral administration and ✲ represent the Log BB values after subcutaneous administration. Based on the indicated classification ranges for PAMPA-BBB, one false positive outlier is obtained.

Table 3
Defined classification ranges for BBB+ and BBB− compounds obtained after evaluation of 19 structurally diverse and commercially available compounds.

	BBB−	BBB+
Log BB	<0	⩾0
PAMPA-BLM	$<2 \times 10^{-6}$ cm/s	$\geqslant 2 \times 10^{-6}$ cm/s
PAMPA-BBB	$<4 \times 10^{-6}$ cm/s	$\geqslant 4 \times 10^{-6}$ cm/s

compounds were tested in a bidirectional Caco-2 assay (Table 4). The obtained efflux ratios of the three false positive outliers showed moderate MDR effects (efflux ratio >2), which suggests that misclassification could be attributed to the effect of p-gp related efflux. Apart from these findings, Figs. 3 and 4 also showed that no significant differences in Log BB values are obtained after

Table 4
J&J Log BB data, in vivo penetration classification and bidirectional Caco-2 data of 14 structurally divers J&J compounds. –: no data available. J&J 9, 12 and 13 are the false positive outliers with the PAMPA-BLM model showing an efflux ratio >2. Only J&J 9 is an outlier with the PAMPA-BBB model.

Compounds	Log BB (PO)	Log BB (SC)	BBB classification	Caco-2 A–B P_{app} (cm/s) 10^{-6}	Caco-2 B–A P_{app} (cm/s) 10^{-6}	Caco-2 efflux ratio
J&J 1	1.04	1.08	BBB+	12.70	42.6	3.4
J&J 2	−1.10	−1.00	BBB−	1.19	3.1	2.6
J&J 3	−0.42	−0.47	BBB−	12.93	21.57	1.7
J&J 4	2.35	2.27	BBB+	48.40	61.30	1.3
J&J 5	0.87	0.82	BBB+	11.10	18.00	1.6
J&J 6	1.37	1.40	BBB+	13.00	24.90	1.9
J&J 7	1.32	1.19	BBB+	22.70	38.40	1.7
J&J 8	1.21	1.07	BBB+	–	–	–
J&J 9	−0.52	−0.52	BBB−	16.97	33.73	2.0
J&J 10	2.02	2.14	BBB+	–	–	–
J&J 11	1.20	1.00	BBB+	11.20	1.57	0.1
J&J 12	−0.22	−0.22	BBB−	8.46	24.53	2.9
J&J 13	−0.15	−0.10	BBB−	13.86	48.10	3.5
J&J 14	1.08	1.20	BBB+	31.50	51.10	1.6

oral administration compared to subcutaneous injection. When relating the PAMPA-BLM P_{eff} vs. the Log BB values after oral administration, the following relationship could be established:

$$\text{PAMPA-BLM } (P_{eff} \times 10^{-6}\ \text{cm/s}) = 8.273 \times \text{Log BB} + 8.201 \quad \text{with} \quad R^2 = 0.731$$

The PAMPA-BBB model classified 13J&J compounds correctly as BBB+ or BBB− compounds (Fig. 4). Only one compound showed a false positive outcome, and this compound was shown to be a substrate for moderate efflux (J&J 9). Although the classification of the J&J compounds is better compared to the PAMPA-BLM model, the obtained relationship generated a slightly worse correlation compared to the PAMPA-BLM model:

$$\text{PAMPA-BBB } (P_{eff} \times 10^{-6}\ \text{cm/s}) = 4.553 \times \text{Log BB} + 4.988 \quad \text{with} \quad R^2 = 0.627$$

Although the PAMPA-DS model and the PAMPA-BBB-UWL model did not differentiate the commercially available compounds as BBB+ or BBB− types, the models were applied to the J&J compounds for the confirmation of the previous observations. Plotting the obtained permeability values vs. the in vivo Log BB values resulted in the following models:

$$\text{PAMPA-DS } (P_{app} \times 10^{-6}\ \text{cm/s}) = 8.876 \times \text{Log BB} + 47.410 \quad \text{with} \quad R^2 = 0.239$$

$$\text{PAMPA-BBB-UWL } (P_{eff} \times 10^{-6}\ \text{cm/s}) = 15.278 \times \text{Log BB} + 10.081 \quad \text{with} \quad R^2 = 0.498$$

The relationships between permeability and Log BB obtained by the PAMPA-DS model and the PAMPA-UWL were characterized by very poor correlations.

4. Conclusions

Both the PAMPA-BLM model, a traditional paradigm for the prediction of GI absorption, and the PAMPA-BBB model predicted the passive diffusion of the J&J compounds reasonably well based on the classification ranges that were established for both models based on the commercially available (training set) compounds. The differences between the artificial lipids (BLM vs. BBB) on the BBB classification of the tested compounds seem to be minimal. With the same experimental conditions, the porcine PBL was more discriminating for BBB+ and BBB− compounds; however, the PAMPA-BLM generated a relationship that better correlated with the Log BB values.

The false positive values obtained in the J&J compound set could be attributed to the compounds being substrates for active efflux. On the other hand, we would like to emphasize that the interpretation of the combined PAMPA and efflux data should be completed with care. Compounds with high efflux ratio can show high (BBB+) in vivo brain penetration due to passive diffusion overcoming the efflux mechanism. We suggest that all compounds with high PAMPA permeability and high efflux ratio be identified as "uncertain" with regard to BBB class. Finally, it is important to recognize that simplistic in vitro models such as PAMPA cannot represent the complicated absorption in the human brain. However, PAMPA data are useful in combination with efflux data and other property data for predicting the ability to penetrate the brain.

Acknowledgments

The authors wish to thank Koen Wuyts and the ADME-tox in vivo group for providing the in vivo Log BB data. Thanks to Chantal Masungi, Pascale Dehertogh, Marleen Van Dooren and An Tuytelaers for their support in the Caco-2 assessment and LC/MS/MS analysis.

References

[1] N.J. Abbott, L. Rönnbäck, E. Hansson, Astrocyte–endothelial interactions at the blood–brain barrier, Nat. Rev. Neurosci. 7 (2006) 41–53.
[2] T.S. Reese, M.J. Karnovsky, Fine structural localization of a blood–brain barrier to exogenous peroxidase, J. Cell Biol. 34 (1967) 207–217.
[3] M.W. Brightman, T.S. Reese, Junctions between intimately apposed cell membranes in the vertebrate brain, J. Cell Biol. 40 (1969) 648–677.
[4] W.M. Pardrige, Brain drug delivery and blood–brain barrier transport, Drug Deliv. 3 (1996) 99–115.
[5] N.J. Abbott, Astrocyte–endothelial interactions and blood–brain barrier permeability, J. Anat. 200 (2002) 629–638.
[6] A. Minn, J.F. Ghersi-Egea, R. Perrin, B. Leininger, G. Siest, Drug metabolizing enzymes in the brain and cerebral microvessels, Brain Res. – Brain Res. Rev. 16 (1991) 65–82.
[7] J. Brownlees, C.H. Williams, Peptidases, peptides, and the mammalian blood–brain barrier, J. Neurochem. 60 (1993) 793–803.
[8] E.A. Brownson, T.J. Abbruscato, T.J. Gillespie, V.J. Hruby, T.P. Davis, Effect of peptidases at the blood brain barrier on the permeability of enkephalin, J. Pharmacol. Exp. Ther. 270 (1994) 675–680.
[9] D. Begley, M.W. Brightman, Structural and functional aspects of the blood–brain barrier, Prog. Drug Res. 61 (2003) 40–78.
[10] C. Cordon-Cardo, J.P. O'Brien, D. Casals, L. Rittman-Grauer, J.L. Biedler, M.R. Melamed, J. R Bertino, Multidrug-resistance gene (P-glycoprotein) is expressed by endothelial cells at blood–brain barrier sites, Proc. Natl Acad. Sci. 86 (1989) 695–698.
[11] S.D. Krämer, N.J. Abbott, D.J. Begley, Biological models to study blood–brain barrier permeation, in: B. Testa, H. van de Waterbeemd, G. Folkers, R. Guy (Eds.), Pharmacokinetic Optimization in Drug Research: Biological, Physicochemical and Computational Strategies, Wiley-VCH, Weinheim, 2001, pp. 127–153.
[12] Y. Deguchi, K. Nozawa, S. Yamada, Y. Yokoyama, R. Kimura R, Quantitative evaluation of brain distribution and blood–brain barrier efflux transport of probenecid in rats by microdialysis: possible involvement of the monocarboxylic acid transport system, J. Pharmacol. Exp. Ther. 290 (1997) 551–560.
[13] H. Sun, D.W. Miller, W.F. Elmquist, Effect of probenecid on fluorescein transport in the central nervous system using in-vitro and in-vivo models, Pharm. Res. 18 (2001) 1542–1549.
[14] H. Takanaga, H. Murakami, N. Koyabu, H. Matsuo, M. Naito, T. Tsuruo, Y. Sawada, Efflux transport of tolbutamide across the blood–brain barrier, J. Pharm. Pharmacol. 50 (1998) 1027–1033.
[15] J. Bentz, T.T. Tran, J.W. Polli, A. Ayrton, H. Ellens, The steady-state Michaelis–Menten analysis of P-glycoprotein mediated transport through a confluent cell monolayer cannot predict the correct Michaelis constant K m, Pharm. Res. 22 (2005) 1667–1677.
[16] B. Gao, B. Stieger, B. Noé, J.M. Fritschy, P.J. Meier, Localization of the organic anion transporting polypeptide 2 (Oatp2) in capillary endothelium and choroid plexus epithelium of rat brain, J. Histochem. Cytochem. 47 (1999) 1255–1263.
[17] S. Cisternino, C. Rousselle, A. Lorico, G. Rappa, J.M. Scherrmann, Apparent lack of mrp1-mediated efflux at the luminal side of mouse blood–brain barrier endothelial cells, Pharm. Res. 20 (2003) 904–909.
[18] T. Eisenblätter, H.J. Galla, A new multidrug resistance protein at the blood–brain barrier, Biochem. Biophys. Res. Commun. 293 (2002) 1273–1278.
[19] S. Cisternino, C. Mercier, F. Bourasset, F. Rouse, J.M. Scherrmann, Expression, upregulation, and transport activity of the multidrug-resistance protein Abcg2 at the mouse blood brain barrier, Cancer Res. 64 (2004) 3296–3301.
[20] P. Breedveld, D. Pluim, G. Cipriani, P. Wielinga, O. van Tellingen, A.H. Schinkel, J.H. Schellens, The effect of Bcrp1 (Abcg2) on the in-vivo pharmacokinetics and brain penetration of imatinib mesylate (Gleevec): implications for the use of breast cancer resistance protein and P-glycoprotein inhibitors to enable the brain penetration of imatinib in patients, Cancer Res. 65 (2005) 2577–2582.
[21] P. Crivori, G. Cruciani, P.-A. Carrupt, B. Testa, Predicting blood–brain barrier permeation from three-dimensional molecular structure, J. Med. Chem. 43 (2000) 2204–2216.
[22] G.F. Ecker, C.R. Noe, In silico prediction models for blood–brain barrier permeation, in: R. Dermietzel, D.C. Spray, M. Nedergaard (Eds.), Blood–brain barriers: from ontogeny to artificial interfaces, vol. 1, Wiley-VCH Verlag GmbH & Co.KGaA, Weinheim, Germany, 2006, pp. 403–428.
[23] J. Mensch, J. Oyarzabal, C. Mackie, P. Augustijns, In vivo, in vitro, and in silico methods for small molecule transfer across the BBB. J. Pharm. Sci. 98 (2009) 4429–4468.

[24] J.A. Nicolazzo, S.A. Charman, W.N. Charman, Methods to assess drug permeability across the blood–brain barrier, J. Pharm. Pharmacol. 58 (2006) 281–293.
[25] P. Garberg, M. Ball, N. Borg, R. Cecchelli, L. Fenart, R.D. Hurst, T. Lindmark, A. Mabondzo, J.E. Nilsson, T.J. Raub, D. Stanimirovic, T. Terasaki, J.O. Oeberg, T. Oesterberg, In-vitro models for the blood–brain barrier, Toxicol. in vitro 19 (2005) 299–334.
[26] A.G. de Boer, P.J. Gaillard, In-vitro models of the blood–brain barrier: when to use which? Curr. Med. Chem. – Cent. Nerv. Syst. Agents 2 (2002) 203–209.
[27] M. Gumbleton, K.L. Audus, Progress and limitations in the use of in-vitro cell cultures to serve as a permeability screen for the blood–brain barrier, J. Pharm. Sci. 90 (2001) 1681–1698.
[28] A. Reichel, D.J. Begley, N.J. Abbott, An overview of in-vitro techniques for blood–brain barrier studies, Methods Mol. Med. 89 (2003) 307–324.
[29] F. Wohnsland, B. Faller, High-throughput permeability pH profile and high-throughput alkane/water log P with artificial membranes, J. Med. Chem. 44 (2001) 923–930.
[30] M. Kansy, F. Senner, K. Gubernator, Physicochemical high throughput screening: parallel artificial membrane permeation assay in the description of passive absorption processes, J. Med. Chem. 41 (1998) 1007–1010.
[31] C. Zhu, L. Jiang, T.M. Chen, K.K. Hwang, A comparative study of artificial membrane permeability assay for high throughput profiling of drug absorption potential, Eur. J. Med. Chem. 37 (2002) 399–407.
[32] C. Masungi, J. Mensch, A. Van Dijck, C. Borremans, B. Willems, C. Mackie, M. Noppe, M.E. Brewster, Parallel artificial membrane permeability assay (PAMPA) combine with a 10-day cell culture as a tool for assessing new drug candidates, Pharmazie 63 (2008) 194–199.
[33] A. Avdeef, Absorption and Drug Development; Solubility, Permeability and the Charged State, John Wiley & Sons, Inc., New Jersey, 2003. pp. 116–246.
[34] D. Galinis-Luciani, L. Nguyen, M. Yazdanian, Is PAMPA a useful tool for discovery? J. Pharm. Sci. 96 (2007) 2886–2892.
[35] A. Avdeef, The rise of PAMPA, Expert Opin. Drug Metab. Toxicol. 1 (2005) 325–342.
[36] A. Avdeef, P. Artusson, S. Neuhoff, L. Lazorova, J. Grasjo, S. Tavelin, Caco-2 permeability of weakly basic drugs predicted with the Double Sink PAMPA method, Eur. J. Pharm. Sci. 24 (2005) 333–349.
[37] E.H. Kerns, L. Di, S. Petusky, M. Farris, R. Ley, P. Jupp, Combined application of parallel artificial membrane permeability assay and Caco-2 permeability assays in drug discovery, J. Pharm. Sci. 93 (2004) 1440–1453.
[38] A. Avdeef, O. Tsinman, PAMPA – a drug absorption in vitro model 13. Chemical selectivity due to hydrogen bonding: in combo comparison of HDM-, DOPC-, and DS-PAMPA, Eur. J. Pharm. Sci. 28 (2006) 43–50.
[39] A. Avdeef, High throughput measurements of permeability profiles, in: H. van de Waterbeemd, H. Lennernäs, P. Artursson (Eds.), Drug Bioavailability, Estimation of Solubility, Permeability, Absorption and Bioavailability, Wiley-VCH, Weinheim, 2003, pp. 46–71.
[40] K. Sugano, N. Takata, M. Machida, K. Saitoh, K. Terada, Prediction of passive intestinal absorption using biomimetic artificial membrane permeation assay and the parallel pathway model, Int. J. Pharm. 241 (2002) 241–251.
[41] H. Liu, C. Sabus, G.T. Carter, C. Du, A. Avdeef, M. Tischler, In vitro permeability of poorly aqueous soluble compounds using different solubilizers in the PAMPA assay with liquid chromatography/mass spectrometry detection, Pharm. Res. 20 (2003) 1820–1826.
[42] C. Dagenais, A. Avdeef, O. Tsinman, A. Dudley, R. Beliveau, P-glycoprotein deficient mouse in situ blood–brain barrier permeability and its prediction using an in combo PAMPA model, Eur. J. Pharm. Sci. 38 (2009) 121–137.
[43] L. Di, E.H. Kerns, I.F. Bezar, S.L. Petusky, Y. Huang, Comparison of blood–brain barrier permeability assays: in situ brain perfusion, MDR1-MDCKII and PAMPA-BBB, J. Pharm. Sci. 98 (2009) 1980–1991.
[44] L. Di, E.H. Kerns, K. Fan, O.J. McConnell, G.T. Carter, High throughput artificial membrane permeability assay for the blood brain barrier, Eur. J. Med. Chem. 38 (2003) 223–232.
[45] E. Deconinck, M.H. Zhang, D. Coomans, Y. Vander Heyden, Classification tree models for the prediction of blood–brain barrier passage of drugs, J. Chem. Inf. Model 46 (2006) 1410–1419.
[46] J. Mensch, M. Noppe, J. Adriaensen, A. Melis, C. Mackie, P. Augustijns, M.E. Brewster, Novel generic UPLC/MS/MS method for high throughput analysis applied to permeability assessment in early Drug Discovery, J. Chromatogr. B 847 (2006) 182–187.
[47] Instruction Manual for PAMPA Evolution Permeability Analyzer, Version 2.2.0, pION Inc., 2004.
[48] A. Avdeef, S. Bendels, L. Di, B. Faller, M. Kansy, K. Sugano, PAMPA – critical factors for better predictions of absorption, J. Pharm. Sci. 96 (2007) 2893–2909.
[49] W.M. Pardridge, Peptide Drug Delivery to the Brain, Raven Press, New York, 1991. pp. 52–88.
[50] D.R. Jones, S.D. Hall, E.K. Jackson, R.A. Branch, G.R. Wilkinson, Brain uptake of benzodiazepines: effects of lipophilicity and plasma protein binding, J. Pharmacol. Exp. Ther. 245 (1988) 816–822.
[51] P.F.C. Bayliss, A.S.M. Duncan, The effects of atenolol (tenormin) and methyldopa on simple tests of central nervous function, Br. J. Clin. Pharmacol. 2 (1975) 527–531.
[52] A.L. McCall, W.R. Millington, R.J. Wurtman, Blood brain barrier transport of caffeine: dose-related restriction of adenine transport, Life Sci. 31 (1981) 2709–2715.
[53] N.O. Martindale, in: J.E.F. Reynolds (Ed.), The Extra Pharmacopoeia, Pharmaceutical Press, London, 1989.
[54] S.K. Kulkarni, A.K. Mehta, J. Kunchandy, Anti-inflammatory actions of clonidine, guanfacine and B-HT 920 against various inflammagen-induced acute paw oedema in rats, Drugs Today 20 (1984) 97–507.
[55] B.B. Hofman, R.J. Lefkowitz, in: J.G. Hardman, L.E. Limbird, P.B. Molinoff, R.W. Ruddon, A.G. Gilman (Eds.), Goodman and Gillmans. The Pharmacological Basis of Therapeutics, ninth ed., McGraw-Hill, New York, 1996, pp. 199–248.
[56] W.M. Scheld, Quinolone therapy for infections of the central nervous system, Rev. Infect. Dis. 11 (1989) S1194–S1202.
[57] P. Jolliet, N. Simon, F. Bree, S. Urien, A. Pagliara, P.A. Carrupt, B. Testa, J.P. Tillement, Pharm. Res. 14 (1997) 650–656.
[58] W.M. Pardridge, Transport of protein-bound hormones into tissues in vivo, Endocr. Rev. 2 (1981) 103–123.
[59] K. Rose, L.H. Hall, L.B. Kier, Modeling blood–brain barrier partitioning using the electrotopological state, J. Chem. Inf. Comp. Sci. 42 (2002) 651–666.